

DISCRIMINATE THE SHORTAGE OF FERTILIZATION AND IRRIGATION FOR LEAFY PLANTS BY USING ALTERNATIVE REPRESENTATIONS OF THE RGB COLOR MODEL

Tarek FOUDA¹, Eltahir MADY², Nouri AL BAY², Shimaa SALAH¹

¹Tanta University, Faculty of Agriculture, Agriculture Engineering Department, Egypt, Emails: tfouda628@gmail.com, Shimaa2010atia@yahoo.com

²Higher Institute of Agricultural Technologies in Al-Ghiran, Tripoli, Libya, E-mails: tahermady312@gmail.com, n.albay60@gmail.com

Corresponding author: tfouda628@gmail.com

Abstract

This study demonstrated the possibility of using the digital image model and Detect The RGB Colour Vegetation Indicators for Cabbage and Lettuce Crop under nitrogen deficiency and water deficiency. For cabbage, the results show the relationship between the vegetation indicators based on colour indicators and the different fertilization levels of cabbage crops, which were at level (50 ETC), indicating that the Hue index and vegetative reached their heights indicators in the fourth level of fertilization (150%) respectively, which amounted to 2.23 and 2.03. While their minimum indicators were the third level of fertilization and amounted to 2.10 and 0.64 respectively. For Lettuce, the results demonstrated the correlation between the color indicators and the fertilization level (0%), which was at level (100% ETC), during the third stage of irrigation. The simple red-green ratio, green-red vegetation index, and visible atmospherically resistant index all reached their maximum indicators on irrigation, amounting to 0.9, 0.84, and 1.07 respectively, while the simple blue-green ratio, green leaf was increasing until it reached 0.22, 0.73, then followed by the normalized green-blue difference whose maximum indicator reached 0.67 in the same period. As a result of irrigation, the RGB-based vegetation indexes 2 and 3 attained their maximum indicators, which were 5.56 and 6.74, respectively. After watering, the Hue index and vegetative indicators attained their respective peak values of 2.23 and 2.81. While their minimum markers were 2.16 and 2, respectively, before irrigation.

Key words: detect, RGB colour, vegetation indicators, cabbage and lettuce, temperature, water, stress, monitoring

INTRODUCTION

A rapid rate of urbanization is expected in the coming years, with approximately 66 percent of the world's population expected to live in urban areas by 2050, compared with 54 percent in 2014. Therefore, 40% of water demand in 2030 is unlikely to be met, and more than 20 percent of arable land is already degraded. Annual cereal production will need to increase by 3 billion tons by 2050 [2]. Lettuce has been counted as a significant functional food because of containing vitamins and minerals [12]. Cabbage is also in the 8th place in production of fresh vegetables with 34,761 and 33,467 tons, respectively in Bursa province in 2014 and 2015 years [19]. Despite the well-known key trends that the future of food and agriculture are facing: such as growing food demand, constraints in natural resources and uncertainties for

agricultural productivity, the projected increase in world population from 7.6 billion in 2018 to well over 9.8 billion in 2050 has received a great deal of attention as an influence on world demand for food [20].

The area planted with vegetables makes up roughly 13% of the area planted with grain crops, whereas the amount of water consumed by vegetables makes up about 20% of the water used for grain crops. The Beijing-Tianjin-Hebei region currently has 58.7% of its vegetable planting area in greenhouses, and greenhouse vegetable planting area, water usage, and fertilizer amount are all rising yearly. According to reports, this region uses 1.3-5.8 times the recommended quantity of nitrogen (N) fertilizer to grow vegetables in greenhouses, and certain areas' groundwater contains more nitrate than others (between 37.5% and 44.8%) [22]. Color can distinguish between different varieties of wheat imported

from different countries. It is also possible to distinguish between Ergot fungi sclerotia and between different types of imported wheat, and the color indicators used showed a clear contrast between wheat and Ergot fungi sclerotia, for example. The physical specifications also showed the differences that distinguish between mushrooms and wheat, which can be used to design the sieve holes for the specific separation. explicates the relationship between Hue and different varieties of wheat and Ergot sclerotia whereas, the ergot French was the highest 0.78 value and the Ukrainian was the lowest 0.47 value. There weren't clear Hue variances between different origin [7]. Here, where the hue value was 0.626, there distinct distinctions between faba bean and soybean. In the faba bean, the intensity and browning index were 91.75 and 16.25, respectively, while in the soybean, they were 0.565, 85.33, and 21.79. While the hue value difference between corn and wheat was only 0.699. Additionally, the intensity and browning index for corn were 100.08 and 17.30, respectively, while these values for wheat were 0.708, 97.94, and 13.38. Additionally, the hue value of 0.634 showed a noticeable difference between cotton and sunflowers. Additionally, the Black & White band and intensity were both 87.40 in cotton while they were 0.480, 96.75, and 96.75 in sunflowers, respectively [1].

Color change for Cowpea seeds after stored effect by FIR and UVC irradiation intensity and hermetic bags (three & seven layers), the differences in Red color band increased by 60.6% when using the seeds that irradiated with UVC radiation and stored in woven bag, utilizing the seeds that had been exposed to FIR radiation and kept in woven bags caused the variations in the green color band to grow by 61.8%. the disparities in the blue color band increased by 65.5% when seeds were stored in woven bags after being exposed to FIR radiation, the differences in Hue increased by 7.14% when using the seeds that irradiated with UVC and stored in three layers bag, the differences in intensity I1 increased by 61.6% when using the seeds that irradiated with FIR and stored in woven bag, the

differences in intensity I2 increased by 60.4% when using the seeds that irradiated with UVC radiation and stored in woven bag and the differences in R/G increased by 9.5% when using in the seeds that irradiated with FIR radiation and stored in three layers bag [8].

Optical sensors have been used to investigate a variety of topics, including: (a) how plants react to pathogens, pests, and abiotic stressors; (b) the identification of primary disease foci; (c) the resistance or susceptibility of various plant genotypes to various stress factors; (d) the severity of symptoms; and (e) the evaluation of plant biomass and yield. One of the most crucial physiological characteristics for plant growth and development is stomatal activity. By regulating transpiration and photosynthesis, it is incredibly important for maintaining the balance of carbon and water. Therefore, stomatal conductance to water (gs), which closely correlates with leaf temperature, is related to yield and to the tolerance of environmental challenges [14]. Examined the integration of TIR cameras with other sensors in phenotyping platforms, such as RGB, multi-, or hyperspectral cameras. To develop reliable approaches for the early diagnosis in crop fields, the discovery of geographical and temporal patterns of TIR parameters in conjunction with other pertinent vegetative indices (VIs) could be very helpful. To identify a stress-specific signature, a preliminary examination of a particular plant-stressor interaction is preferred [16].

Thermography-Based Biotic Stress Detection at Various Scales Stomatal closure typically occurs when a possible pathogen is detected by plants, however some pathogens have the ability to bypass the plant's signaling pathways and activate stomatal aperture instead. Other consequences of pathogen infection include changes in the metabolism, necrosis of the tissues, cell wall and leaf cuticle compositional or structural changes, and abnormalities in leaf growth. The water status of the plant is impacted by these physical and chemical disturbances, and thermography can be used to monitor it [17]. Plant monitoring form an important part of the agriculture and horticulture sectors in

our country as they can be used to grow plants under controlled climatic conditions for optimum produce. Automating a plant monitoring and controlling of the climatic parameters which directly or indirectly govern the plant growth and hence their produce. Automation is process control of industrial machinery and processes, thereby replacing human operators [15].

Summarized and discussed the benefits and limitations of phenotyping imaging methods (RGB, multispectral, and hyperspectral sensors, among others) that have been used to evaluate various abiotic stresses, such as salinity, drought, and nitrogen deficit. Here, we provide a thorough analysis of the features related to abiotic tolerance that have been measured using a variety of image sensors in high-throughput phenotyping labs or by unmanned aerial vehicles in the field. We also examine the advancement and difficulties in machine learning, including supervised and unsupervised models as well as deep learning, and present a current compilation of spectral tolerance indexes [3].

The results confirmed the possibility of pre-symptomatic detection of *P. carotovorum* subsp. *carotovorum* in lettuce at the canopy level. With respect to identifying healthy and infected lettuce plants by supervised classification, the best results were obtained at 4 and 8 DAI, especially when using the subsets derived from the Mapir Survey3W camera (RGN sensor), for both classifiers. The subsets obtained with the conventional visible sensor (RGB sensor) produced the best results at 20 and 24 days[5].

The main objectives of this study using the digital image model and Detect The RGB Color Vegetation Indicators for Cabbage and Lettuce Crop under nitrogen deficiency and water deficiency.

MATERIALS AND METHODS

Cabbage and lettuce seed, greenhouse, soil, and water, Phosphoric, Nitrogen fertilizer, and Canon ESO R. 4000 digital camera with MATLAB program as a materials were used under this study. The RGB colour model and digital camera, using the capture card to

transferred the data and stored on the PC. MATLAB software package was used to analysed the digital images as showed in RGB monitoring system (Photo 1).

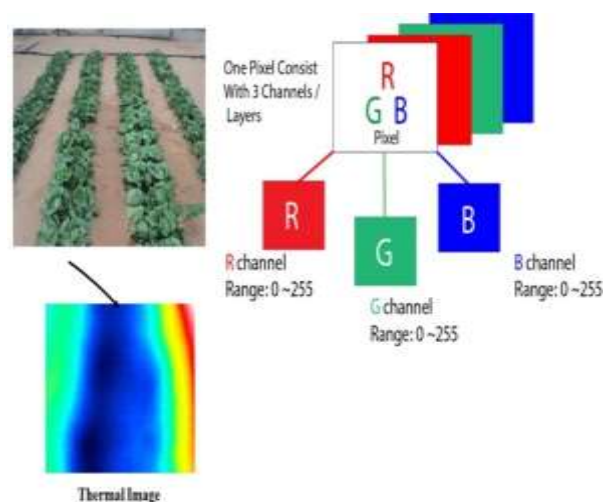


Photo 1. RGB monitoring system
Source: Authors' determination.

The digital camera

The Canon ESO R. With a DIGIC 8 image processor and a high-resolution 26.2MP full-frame CMOS sensor, still images and UHD 4K video can be captured with a wide sensitivity range, from ISO 100 to 40000, to accommodate working in a variety of lighting settings. For taking pictures of moving subjects, continuous shooting at up to 5 fps is also enabled. Additionally, the sensor enables a cutting-edge Dual Pixel CMOS AF system with 4,779 configurable on-sensor phase-detection points for fast and precisely focusing both stills and video operation(Photo 2).



Photo 2. The digital camera - Canon ESO R.
Source: From catalogue.

Photo 2 and Table 1 show and explain the Canon ESO R.

Table 1. The specification of digital camera - Canon ESO R

Brand	Canon
Effective still resolution	26.2 MP
Screen size	7.5 Centimeters
Item weight	440 Grams

Source: From catalogue.

MATLAP PC-Software

For Image Analysis system it was used MATLAB program. Samples were captured by digital camera, using the capture card to

transferred the data and stored on the PC. The MATLAB software package was used to analyzed the images of Cabbage and lettuce. There were three bands, RGB, were derived for each image until obtaining color indices.

User interface

MATLAB Interface have many items ribbon, work space and status bar to detect image. Photo 3 Envi program interface, ribbon, work space and status bar.

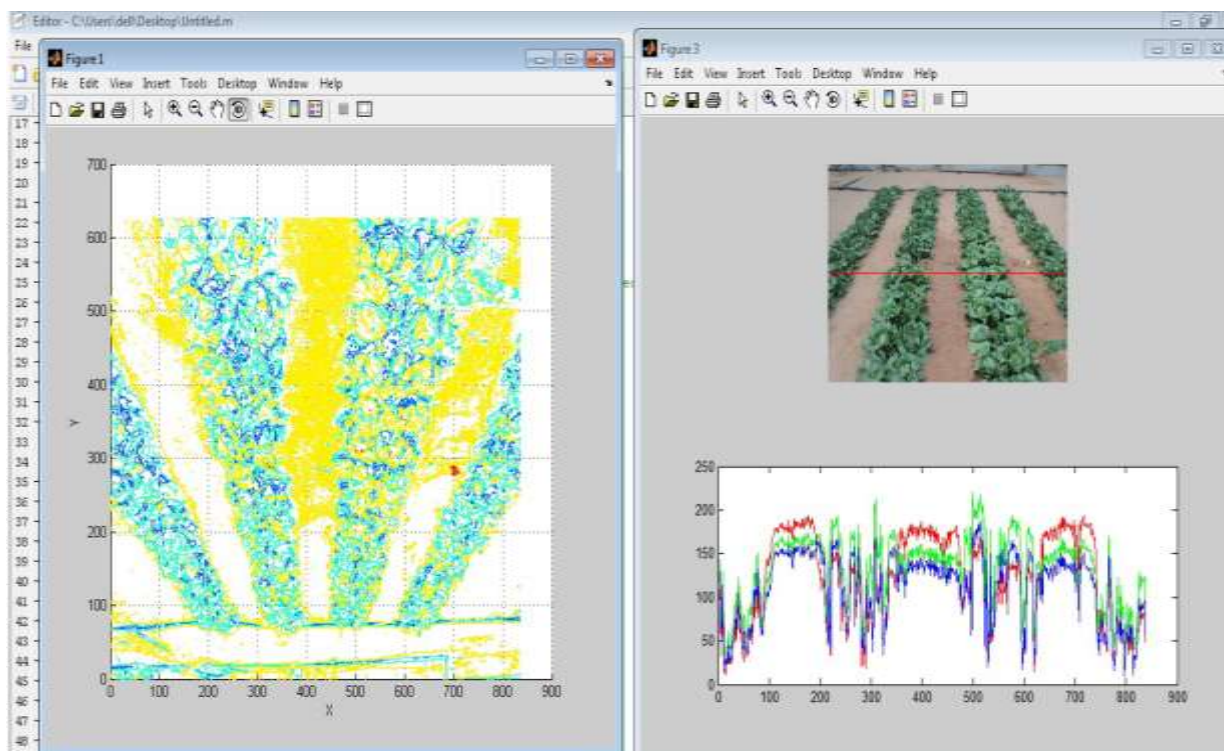


Photo 3. MATLAB interface, ribbon, work space and status bar
 Source: Authors' determination.

Vegetation Indices Basics RGB

A Vegetation Index is a single value calculated by transforming the observations from multiple RGB bands.

It is used to enhance the presence of green, vegetation features and thus help to distinguish them from the other objects present in the image.

Depending on the transformation method and the RGB bands used, different aspects pertaining to the vegetation cover in the image could be evaluated say, the percentage of vegetation cover, amount of chlorophyll content, leaf area index and so on.

All the ratio indexes, in general, are independent of the illumination conditions at the time of acquisition and slope effects.

Simple Ratio (SR)

This is a ratio between the reflectance recorded in the RGB bands as shown in Table 2.

This is a simple method for separating green leaves from other scene elements and determining the relative biomass that is visible.

Additionally, this value might be very helpful in differentiating between stressed and non-stressed vegetation.

Table 2. RGB bands vegetation indices

Acronym	Indices	Definition	Author and Year
GR	Simple red-green ratio	$\frac{R}{G}$	Gamon et al., 1999[9]
GRVI	Green-red vegetation index	$\frac{G - R}{G + R}$	Tucker et al., 1979[18]
RGBVI	RGB-based vegetation index	$\frac{G^2 - (BXR)}{G^2 + (BXR)}$	Bendig et al., 2015[4]
MGRVI	Modified green-red vegetation index	$\frac{G^2 - R^2}{G^2 + R^2}$	Bendig et al., 2015[4]
VARI	Visible atmospherically resistant index	$\frac{G - R}{G + R - B}$	Gitelson et al., 2002[10]
BGI2	Simple blue-green ratio	$\frac{B}{G}$	Zarco-Tejada et al., 2005[23]
VEG	Vegetative	$\frac{G}{R^2XB^{(1-a)}} ; a = 0.667$	Hague et al., 2006[11]
GLI	Green leaf	$\frac{2G - R - B}{2G + R + B}$	Woebbecke et al., 1995[21]
ExG	Excess green index	$2G-R-B$	Du et al., 2017[6]
NGBDI	Normalized green-blue difference index	$\frac{G - B}{G + B}$	Du et al., 2017[6]
RGBVI2	RGB-based vegetation index 2	$\frac{G - R}{B}$	Proposed
RGBVI3	RGB-based vegetation index 3	$\frac{G + B}{R}$	Proposed
VARI	Visible Atmospheric Resistant Index	$VARI = \frac{green-Red}{green+Red-blue}$	Gitelson et al., 2002[10]
Hue	Hue	$H = \cos^{-1} \left(\frac{(2R-G-B)/2}{(R-G)^2 + (R-B)(2G-B)^{0.5}} \right)$	Khojastehnazhand et al., 2009[13]
I	Intensity	$I = \frac{1}{3}(R+G+B)$	
I ₂	Intensity-	$I_2 = (R-B)/2$	

Source: Authors' determination based on the studied literature. [4], [6], [9], [10], [11], [13], [18], [21] and [23].

C++ plus model

The C++ programming language was used to build a set of algorithms to determine and predict the colorimetric indicators and to research the effects of water and fertilizer scarcity. The C++-written simulation and forecasting programs.

The program model test in this study the two Cabbage and lettuce seed in greenhouse, with sand soil, and water, Phosphor, Nitrogen fertilizer, using digital and thermal camera with MATLAB and IR soft program the programs flowchart model steps showed below in the coming Figures.

ColorVegetation (CVI) Program model I

using this technique to estimate the color indices to distinguish the vegetative

characteristics using alternative representations of the RGB Color Model Simulation and predicting programs model written by C++ to estimate the color calcification indices as showing in Figures 1 and 2.

-In put: RGB band color

-Calculate: I₂ and I₂ stand for hue, value, and saturation. ratio of red to green, a straightforward red-green ratio, a modified green-red vegetation index, an RGB-based vegetation index, visible index of atmospheric resistance, straightforward blue-green ratio Green leaf, RGB-based vegetation index, normalized green-blue difference index, excess green index, and vegetative 2

Vegetation Index based on RGB The Visible Atmospheric Resistant Index is three.

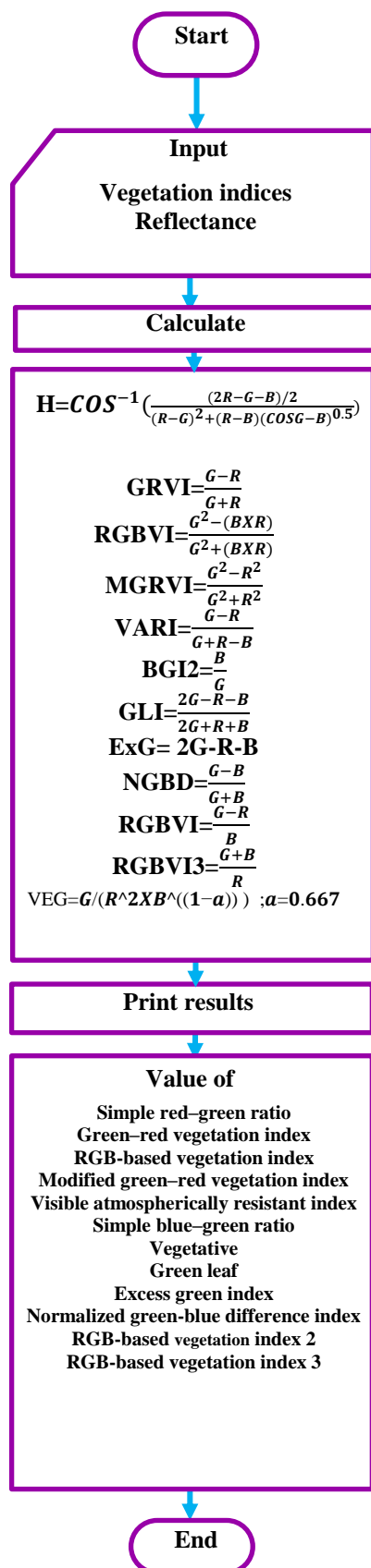


Fig. 1. Flowchart of Color Vegetation indices (CVI) program model I
 Source: Authors' drawing.

-Predicting and determined Color indices to monitoring toxic and protecting from plant stresses

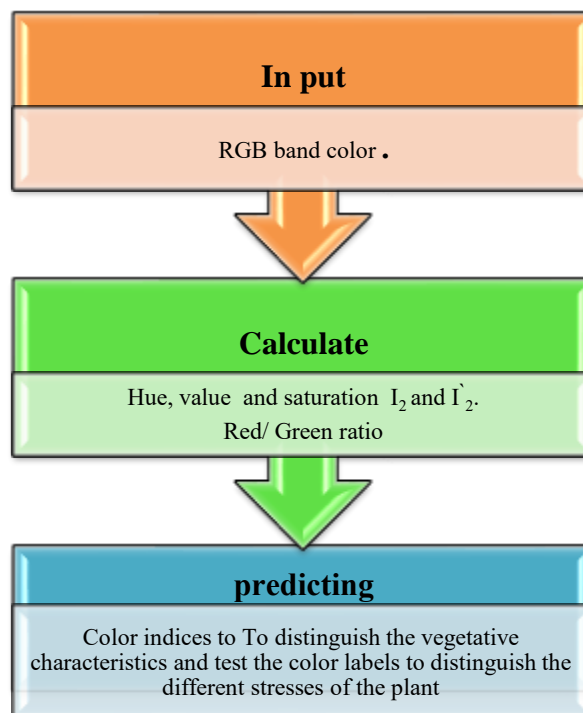


Fig. 2. Sequence for Color indices predictions to distinguish the vegetative characteristics and different stresses of the plant

Source: Authors' drawing

RESULTS AND DISCUSSIONS

Detecting By Digital Imaging For Monitoring Cabbage And Lettuce Crop At Late Season Stage Growth Periods

The digital imaging for showing plants monitoring data collecting to express about different levels of water regime and nitrogen fertilization with at late season stage growth periods. Red and blue bands, Hue, VEG, the simple red-green ratio, green-red and all vegetation index were tested to monter the effect different fertilization and irrigation levels. Monitoring RGB Color Indices With Fertilization And Irrigation Levels For Cabbage And Lettuce Crop.

Figure 3 with the levels of fertilization showed the maximum value of Hue and vegetative which were 2.36. and 2.61, also showed the minimum value for the same indices were 2.16 and 1.21. Linear regression analysis was performed, to predict the monitoring Hue and vegetative at different

fertilization levels. The following equation represents the relationship.

$$\text{Hue: } y = 0.068x + 2.105 \quad R^2 = 0.9593$$

$$\text{Vegetative: } y = 0.4446x + 0.7212 \quad R^2 = 0.9511$$

Figure 4 with the levels of fertilization showed the maximum value of simple red-green ratio and Green-red vegetation index which was 0.16. and 0.83, and also showed the minimum value for the same indices were 0.12 and 0.74. Linear regression analysis was performed to predict the red-green ratio and Green-red vegetation index at different fertilization levels. The following equation represents the relationship.

$$\text{GR: } y = 0.0124x + 0.1135 \quad R^2 = 0.902$$

$$\text{GRVI: } y = 0.0293x + 0.178 \quad R^2 = 0.9627$$

The simple blue-green ratio and the visible atmospherically resistant index had maximum values of 0.99 and 0.29, respectively, and minimum values of 0.92 and 0.16, respectively, in Figure 5 with the amounts of fertilization.

The visible atmospherically resistant index and the blue-green ratio at various fertilization amounts were predicted using a linear regression analysis.

The following equation represents the relationship.

$$\text{BGI2: } y = 0.0205x + 0.9134 \quad R^2 = 0.9324$$

$$\text{VARI: } y = 0.0437x + 0.1235 \quad R^2 = 0.9598$$

The same trend accrued with simple green leaf and normalized green-blue difference index color indices, as Figure 6 expressed by

$$\text{GLI: } y = 0.0397x + 0.5571 \quad R^2 = 0.9083$$

$$\text{NGBDI: } y = 0.0361x + 0.6201 \quad R^2 = 0.9811$$

Also, RGB-based vegetation index 2 and RGB-based vegetation index 3 at Figure 7 with different fertilization levels expressed by:

$$\text{RGBVI2: } y = 0.7478x + 4.0979 \quad R^2 = 0.958$$

$$\text{RGBVI3: } y = 0.6999x + 2.8577 \quad R^2 = 0.9441$$

Figure 8 with the levels of irrigation showed the maximum value of Hue and vegetative which were 2.33. and 3.55, and also showed the minimum value for the same indices which were 2.16 and 1.7. Linear regression analysis was performed to predict the monitoring Hue and vegetative at different irrigation levels. The following equation represents the relationship.

$$\text{Hue: } y = 0.0571x + 2.0957 \quad R^2 = 0.9646$$

$$\text{Vegetative: } y = 0.6398x + 1.0704 \quad R^2 = 0.9881$$

The simple red-green ratio and the Green-red vegetation index in Figure 9 with the levels of irrigation indicated their highest values to be 0.26 and 0.85 respectively, as well as their minimum values to be 0.15 and 0.7. To forecast the monitoring simple red-green ratio and the green-red vegetation index at various irrigation levels, linear regression analysis was used. The relationship is represented by the equation below.

$$\text{GR: } y = 0.0375x + 0.1073 \quad R^2 = 0.9863$$

$$\text{GRVI: } y = 0.0544x + 0.6427 \quad R^2 = 0.9755$$

The simple blue-green ratio and the visible atmospherically resistant index had maximum values of 0.25 and 1.19, respectively, and minimum values of 0.19 and 0.85, respectively, in Figure 10 with the degrees of irrigation. The monitoring simple blue-green ratio and visible atmospherically resistant index at various irrigation levels were predicted using a linear regression analysis. The following equation represents the relationship.

$$\text{BGI2: } y = 0.0216x + 0.165 \quad R^2 = 0.9507$$

$$\text{VARI: } y = 0.1225x + 0.715 \quad R^2 = 0.9522$$

The normalized green-blue difference index and green leaf maximum values were 0.76 and 0.74, respectively, in Figure 11. The normalized green-blue minimum values were 0.64 and 0.65, respectively. To forecast the monitoring's green leaf and normalized green-blue difference index at various irrigation levels, linear regression analysis was used. The relationship is depicted by the following equation.

$$\text{GLI: } y = 0.0405x + 0.6084 \quad R^2 = 0.9789$$

$$\text{NGBDI: } y = 0.0306x + 0.6265 \quad R^2 = 0.9481$$

The RGB-based vegetation index 2 and RGB-based vegetation index 3 had maximum values of 5.21 and 6.79, respectively, and minimum values of 4.25 and 5.15, respectively, in Figure 12 with the degrees of irrigation. Linear regression analysis was performed to predict the monitoring RGB-based vegetation index 2 and RGB-based vegetation index 3 at different irrigation levels. The following equation represents the relationship.

$$\text{RGBVI2: } y = 0.3088x + 3.915 \quad R^2 = 0.965$$

$$\text{RGBVI3: } y = 0.5311x + 4.5624 \quad R^2 = 0.9917$$

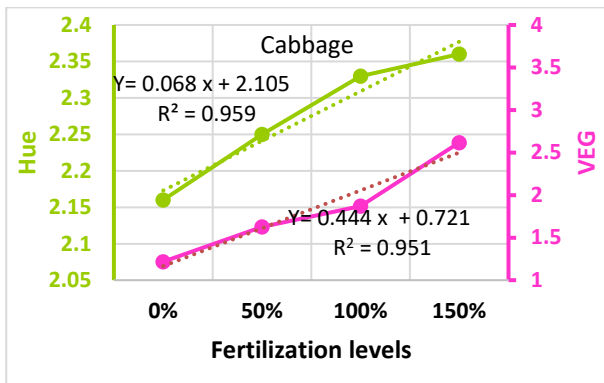


Fig. 3. The Hue and Vegetative Color Indices of the Cabbage Crop in Relation to Fertilization Levels
 Source: Authors' determination.

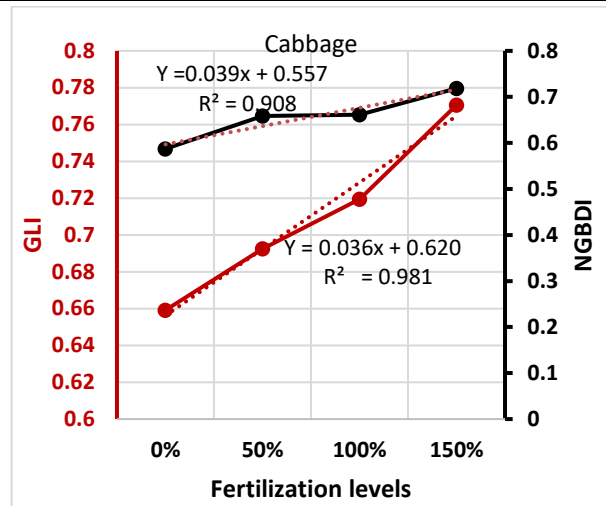


Fig. 6. The normalized green-blue difference index and basic green leaf color indices with cabbage crop fertilizer levels
 Source: Authors' determination.

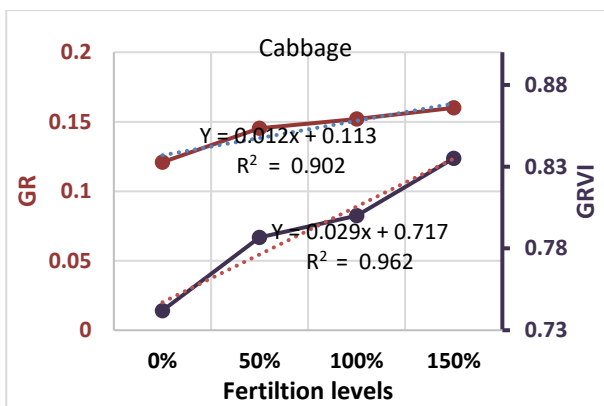


Fig. 4. The straightforward red-green ratio and the green-red vegetation index are color indices that correlate with the fertilization rates of cabbage crops.
 Source: Authors' determination.

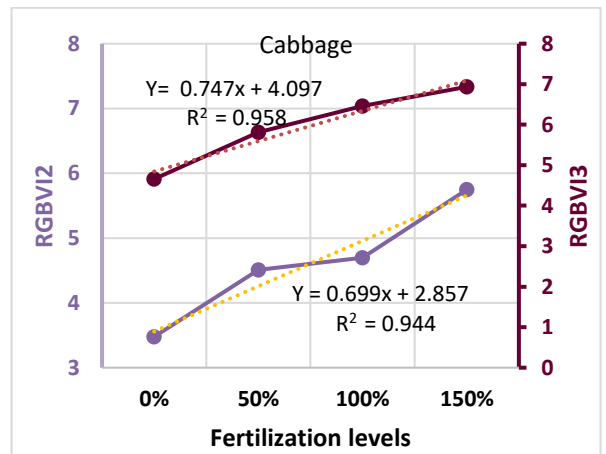


Fig. 7. The RGB-based vegetation index 2 and 3 color indices with levels of fertilizer in the cabbage crop
 Source: Authors' determination.

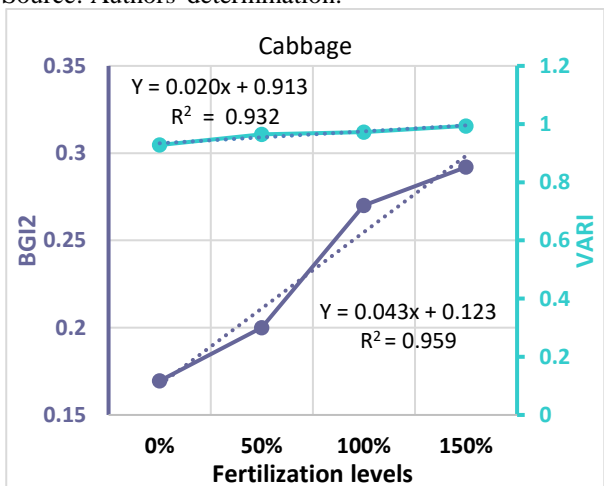


Fig. 5. The straight forward blue-green ratio and visible atmospheric resistance index color indices with cabbage crop fertilizer levels
 Source: Authors' determination.

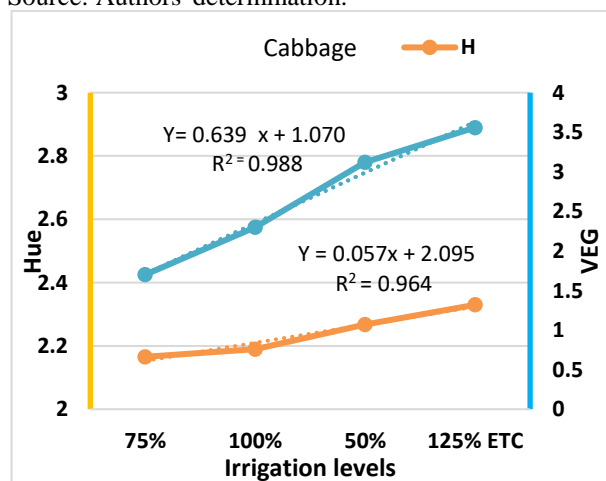


Fig. 8. The hue and vegetative color indices with irrigation levels of the cabbage crop at the first level of fertilization
 Source: Authors' determination.

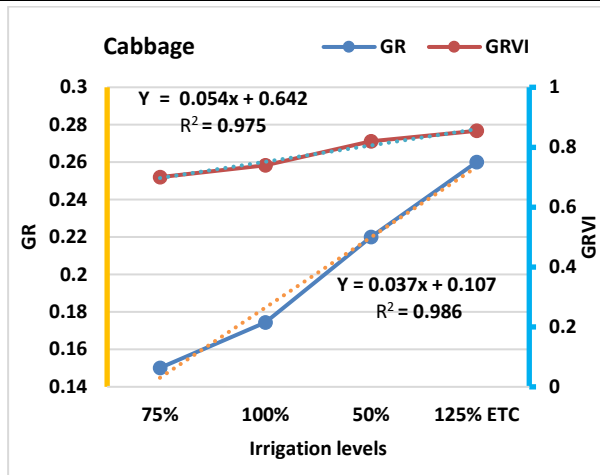


Fig. 9. The straight forward red-green ratio and the green-red vegetation index, along with the cabbage crop's irrigation levels at the first level of fertilization, are color indices.
 Source: Authors' determination.

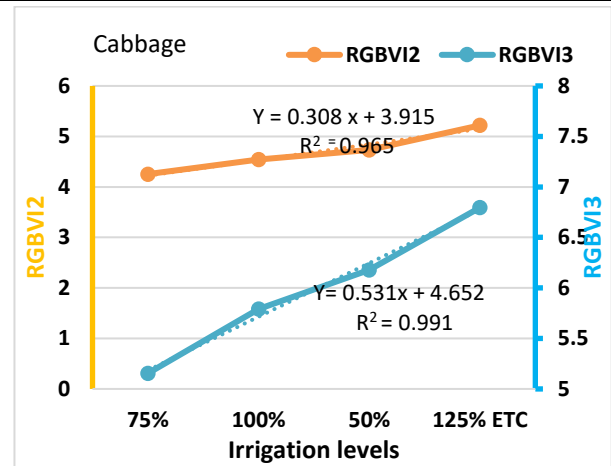


Fig. 12. The RGB-based vegetation index 2 and 3 color indices with cabbage crop irrigation levels at the first phase of fertilization
 Source: Authors' determination.

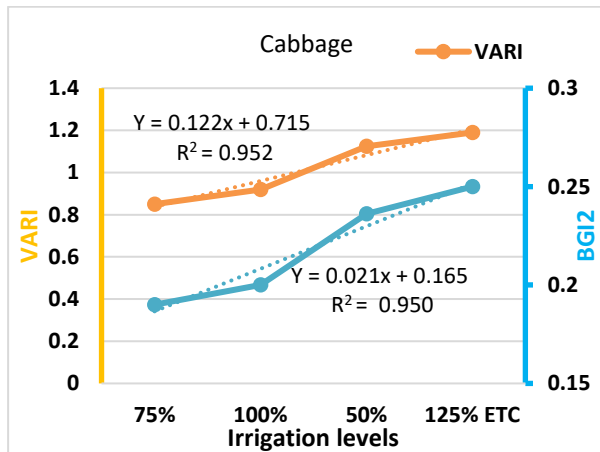


Fig. 10. The straightforward blue-green ratio, visible atmospheric resistance indices, and cabbage crop irrigation levels at the first stage of fertilizing
 Source: Authors' determination.

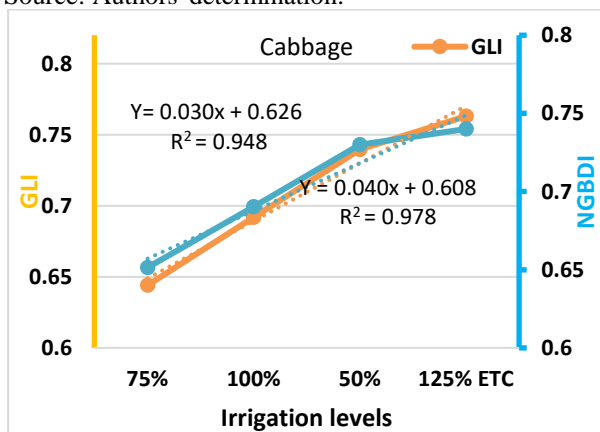


Fig. 11. Using irrigation levels of the cabbage crop at the first level of fertilization, the simple green leaf and normalized green-blue difference index color indices were calculated.
 Source: Authors' determination.

Figure 13 with the levels of fertilization showed the maximum value of Hue and vegetative which were 2.22. and 2.44, and also showed the minimum value for the same indices which were 2.16 and 1.37. Linear regression analysis was performed to predict the monitoring Hue and vegetative at different fertilization levels. The following equation represents the relationship.

Hue: $y = 0.018x + 2.1426$ $R^2 = 0.9233$

Vegetative: $y = 0.3514x + 0.943$ $R^2 = 0.9462$

The basic red-green ratio and the Green-red vegetation index in Figure 14 with the levels of fertilization indicated their maximum values to be 0.18 and 0.83 and 0.12 and 0.74, respectively. At various fertilization amounts, the red-green ratio and the green-red vegetation index were predicted using a linear regression analysis. The following equation represents the relationship.

GR: $y = 0.0321x + 0.0562$ $R^2 = 0.9849$

GRVI: $y = 0.0322x + 0.6977$ $R^2 = 0.9305$

The simple blue-green ratio and the visible atmospherically resistant index had maximum values of 0.99 and 0.3 in Figure 15 with the levels of fertilization, and minimum values of 0.92 and 0.169, respectively. The visible atmospherically resistant index and the blue-green ratio at various fertilization amounts were predicted using a linear regression analysis. The following equation represents the relationship.

BGI2: $y = 0.023x + 0.901$ $R^2 = 0.9742$

VARI: $y = 0.0454x + 0.1227$ $R^2 = 0.9829$

The normalized green-blue difference index and green leaf maximum values were 0.77 and 0.8, respectively, in Figure 16. The normalized green-blue difference index and green leaf minimum values were 0.58 and 0.65, respectively. The normalized green-blue difference index and the green leaf were predicted using linear regression analysis at various fertilization levels. The following equation represents the relationship.

$$\text{GLI: } y = 0.059x + 0.5314 \quad R^2 = 0.9904$$

$$\text{NGBDI: } y = 0.045x + 0.6054 \quad R^2 = 0.9321$$

The RGB-based vegetation index 2 and RGB-based vegetation index 3 were shown to have maximum values of 7.7 and 6, respectively, and minimum values of 4.65 and 3.47, respectively, in Figure 17 with the amounts of fertilization. The RGB-based vegetation index 2 and RGB-based vegetation index 3 were predicted using linear regression analysis at various fertilization amounts. The following equation represents the relationship.

$$\text{RGBVI2: } y = 0.9773x + 3.7155 \quad R^2 = 0.9871$$

$$\text{RGBVI3: } y = 0.826x + 2.7314 \quad R^2 = 0.9932$$

Figure 18 with the levels of irrigation showed the maximum value of Hue and vegetative which were 2.23. and 1.63, and also showed the minimum value for the same indices which were 2.11 and 1. Linear regression analysis was performed to predict the monitoring Hue and vegetative at different irrigation levels. The following equation represents the relationship.

$$\text{Hue: } y = 0.0365x + 2.0811 \quad R^2 = 0.9589$$

$$\text{Vegetative: } y = 0.194x + 0.8343 \quad R^2 = 0.9859$$

The RGB-based vegetation index 2 and RGB-based vegetation index 3 were shown to have maximum values of 7.7 and 6, respectively, and minimum values of 4.65 and 3.47, respectively, in Figure 19 with the amounts of fertilization. The RGB-based vegetation index 2 and RGB-based vegetation index 3 were predicted using linear regression analysis at various fertilization amounts. The following equation represents the relationship.

$$\text{GR: } y = 0.026x + 0.0418 \quad R^2 = 0.9924$$

$$\text{GRVI: } y = 0.0233x + 0.6864 \quad R^2 = 0.9588$$

The simple blue-green ratio and the visible atmospherically resistant index had maximum values of 0.26 and 1, respectively, and minimum values of 0.16 and 0.85,

respectively, in Figure 20 with the degrees of irrigation. The monitoring simple blue-green ratio and visible atmospherically resistant index at various irrigation levels were predicted using a linear regression analysis. The following equation represents the relationship.

$$\text{BGI2: } y = 0.0299x + 0.1339 \quad R^2 = 0.9544$$

$$\text{VARI: } y = 0.0523x + 0.8013 \quad R^2 = 0.9011$$

The normalized green-blue difference index and the maximum and minimum values for those indices, respectively, for Figure 21 with the levels of irrigation, were 0.69 and 0.65 respectively. To forecast the normalized green-blue difference index and monitoring green leaf at various irrigation levels, linear regression analysis was used. The following equation represents the relationship.

$$\text{GLI: } y = 0.0127x + 0.6499 \quad R^2 = 0.9448$$

$$\text{NGBDI: } y = 0.0342x + 0.5214 \quad R^2 = 0.9765$$

The RGB-based vegetation index 2 and RGB-based vegetation index 3 were shown to have maximum values of 4.25 and 5.67 in Figure 22 along with their respective minimum values of 3.22 and 4.54. The monitoring RGB-based vegetation index 2 and RGB-based vegetation index 3 at various irrigation levels were predicted using a linear regression analysis. The following equation represents the relationship.

$$\text{RGBVI2: } y = 0.3536x + 2.8756 \quad R^2 = 0.9909$$

$$\text{RGBVI3: } y = 0.3866x + 4.0409 \quad R^2 = 0.9398$$

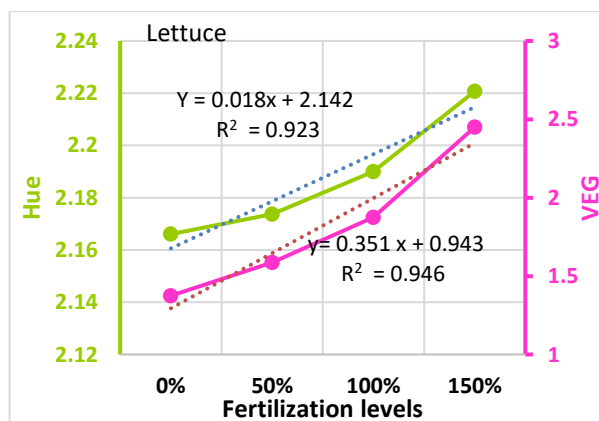


Fig. 13. The Hue and vegetative color indices with fertilization levels of lettuce crop
 Source: Authors' determination.

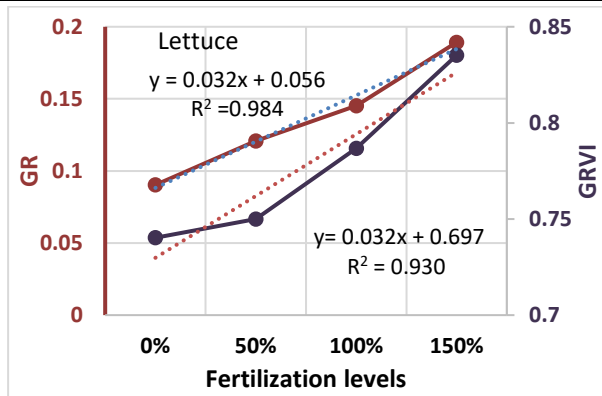


Fig. 14. The simple red–green ratio and Green–red vegetation index color indices with fertilization levels of lettuce crop

Source: Authors' determination.

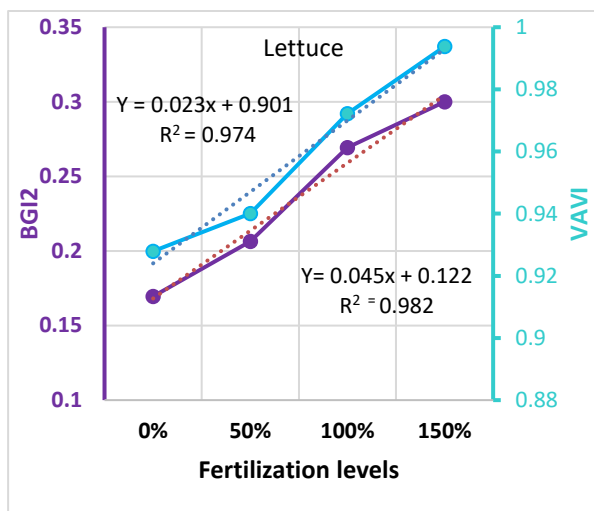


Fig. 15. The straightforward blue–green ratio and visible atmospheric resistance index color indices with lettuce crop fertilizer levels

Source: Authors' determination.

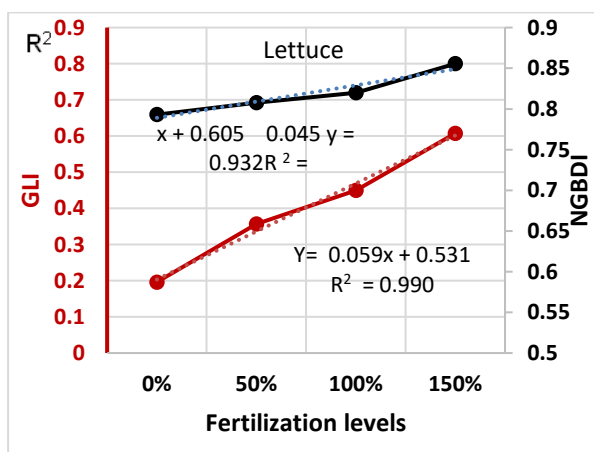


Fig. 16. The normalized green–blue difference index and basic green leaf color indices with lettuce crop fertilization levels

Source: Authors' determination.

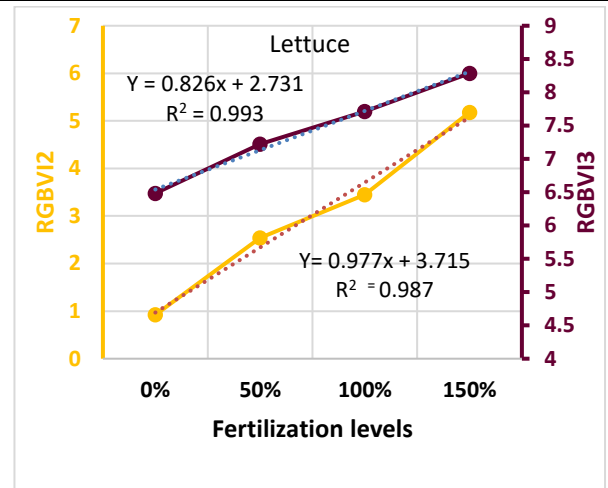


Fig. 17. The color indices for the RGB-based vegetation index 2 and 3 with lettuce crop fertilization levels

Source: Authors' determination.

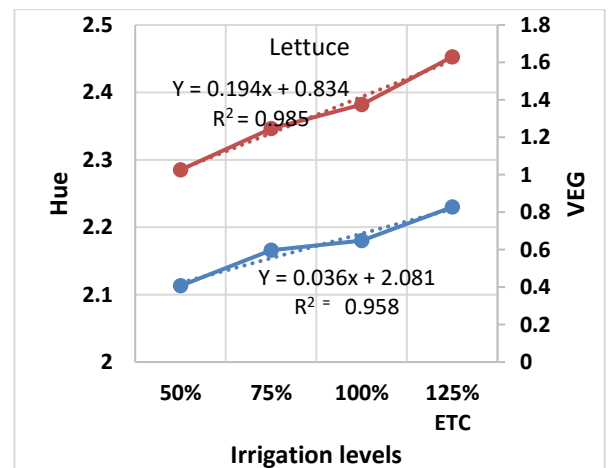


Fig. 18. The lettuce crop's hue and vegetative color indices and irrigation levels

Source: Authors' determination.

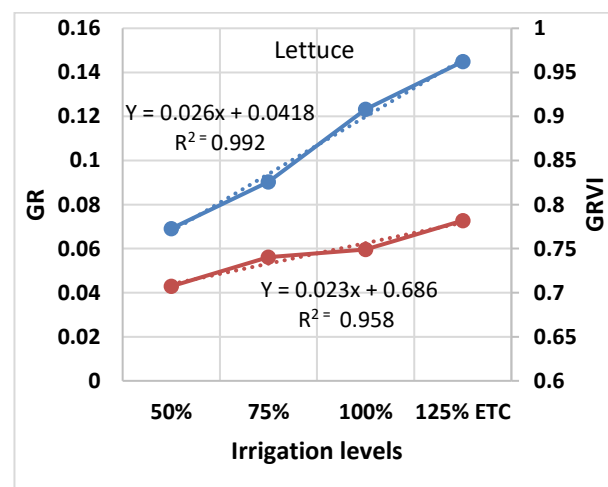


Fig. 19. The simple red–green ratio and the green–red vegetation index, along with the lettuce crop's watering levels

Source: Authors' determination.

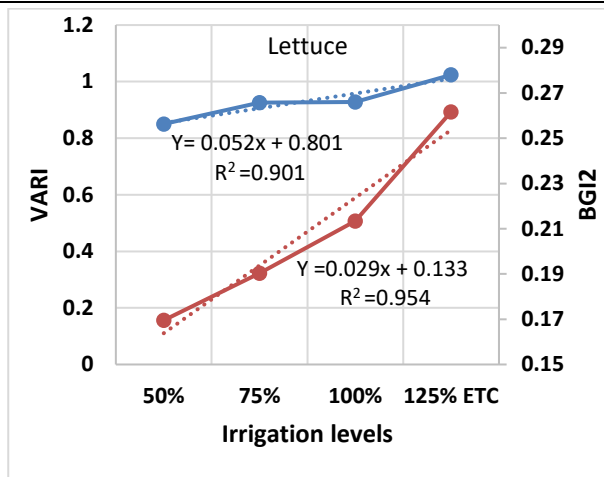


Fig. 20. The straight forward blue-green ratio and readily observable atmospheric resistance color indices with lettuce crop irrigation levels
 Source: Authors' determination.

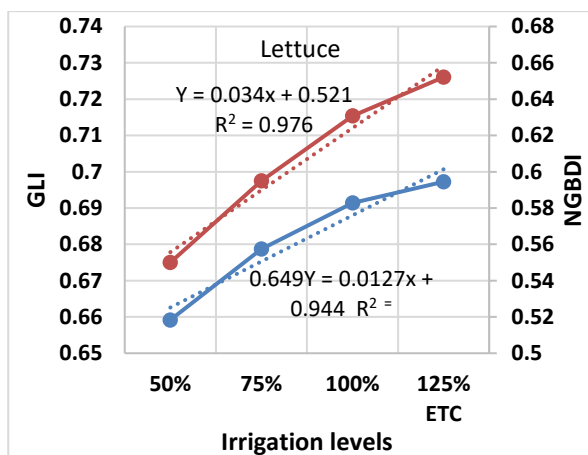


Fig. 21. The normalized green-blue difference index and simple green leaf color indices with lettuce crop irrigation levels
 Source: Authors' determination.

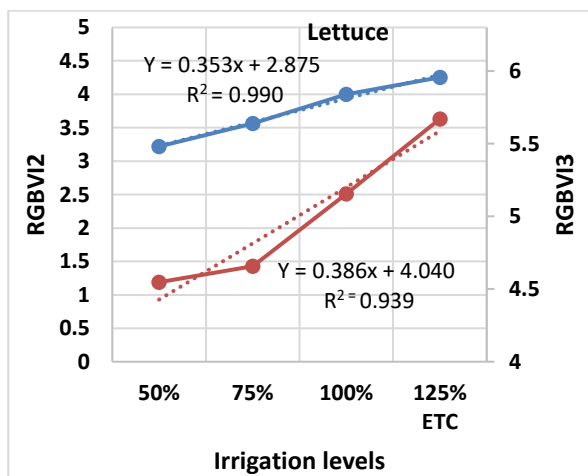


Fig. 22. The color indices for the RGB-based vegetation index 2 and 3 with lettuce crop irrigation levels
 Source: Authors' determination.

CONCLUSIONS

To distinguish between the lack of irrigation and fertilization for leafy plants, a digital image form can be used. Detection of the RGB-colored vegetation indicators for lettuce and cabbage crops that are suffering from a nitrogen and water shortage. There was a significant association between the various amounts of fertilization and irrigation and the vegetation cover indicators based on color indicators.

REFERENCES

- [1]Abdelsalam, A., Foauda, T., 2023, Determination of color properties of some seeds. Scientific Papers. Series "Management, Economic Engineering in Agriculture and rural development", Vol. 23(1), 15-20. Accessed on 8/10/2023.
- [2]Alexandratos, N., Bruinsma, J., 2012, World agriculture towards 2030/2050: the 2012 revision. ESA Working Paper No. 12-03. Rome, FAO.
- [3]Al-Tamimi, N., Langan, P., Bernád, V., Walsh, J., Mangina, E., Negrão, S., 2022, Capturing crop adaptation to abiotic stress using image-based technologies. Open Biology, 12(6), 210353. Accessed on 8/10/2023.
- [4]Bendig, J., Yu, K., Aasen, H., Bolten, A., Bennertz, S., Broscheit, J., Gnyp, M.L., Bareth, G., 2015, Combining UAV-based plant height from crop surface models, visible, and near infrared vegetation indices for biomass monitoring in barley. International Journal of Applied Earth Observation and Geoinformation, 39, pp. 79-87. Accessed on 8/10/2023.
- [5]Carmo, G. J. D. S., Castoldi, R., Martins, G. D., Jacinto, A. C. P., Tebaldi, N. D., Charlo, H. C. D. O., Zampiroli, R., 2022, Detection of Lesions in Lettuce Caused by *Pectobacterium carotovorum* Subsp. *carotovorum* by Supervised Classification Using Multispectral Images. Canadian Journal of Remote Sensing, 48(2), 144-157. Accessed on 8/10/2023.
- [6]Du, M., Noguchi, N., 2017, Monitoring of wheat growth status and mapping of wheat yield's within-field spatial variations using color images acquired from UAV-camera system. Remote sensing, 9(3), 289. Accessed on 8/10/2023.
- [7]Fouda, T., Albabany, A., 2021, Using alternative representations of the RGB color model to separate *Ergot Sclerotia (Claviceps purpurea)* from the imported wheat, Scientific Papers. Series "Management, Economic Engineering in Agriculture and rural development", Vol. 21(1), 337-344. Accessed on 8/10/2023.
- [8]Fouda, T., El-Kholy, M., Elmetwalli, A., Slaeh, D., Salah, S., 2021, Monitoring changes in Cowpea color and storage conditions. Scientific Papers. Series "Management, Economic Engineering in Agriculture

- and rural development", Vol. 21(4), 243-252. Accessed on 8/10/2023.
- [9]Gamon, J. A., Surfus, J. S., 1999, Assessing leaf pigment content and activity with a reflectometer. *The New Phytologist*, 143(1), 105-117. Accessed on 8/10/2023.
- [10]Gitelson, A. A., Kaufman, Y. J., Stark, R., Rundquist, D. (2002). Novel algorithms for remote estimation of vegetation fraction. *Remote Sensing of Environment*, 80(1), 76-87. Accessed on 8/10/2023.
- [11]Hague, T., Tillett, N. D., Wheeler, H., 2006, . Automated crop and weed monitoring in widely spaced cereals. *Precision Agriculture*, 7, 21-32. Accessed on 8/10/2023.
- [12]Jones, H., 2014, *Plants and Microclimate: A Quantitative Approach to Environmental Plant Physiology*, 3rd ed.; Cambridge University Press: Cambridge, UK, 2014, Vol. 56. Accessed on 8/10/2023.
- [13]Khojastehnazhand, M., Omid, M., Tabatabaefar, A., 2009, Determination of orange volume and surface area using image processing technique. *International Agrophysics*, 23(3), 237-242. Accessed on 8/10/2023.
- [14]Kim, M.J., Moon, Y., Tou, J.C., Mou, B., Waterland, N.L., 2016, Nutritional value, bioactive compounds and health benefits of lettuce (*Lactucasativa* L.). *J Food Compos Anal* 49:19–34. <https://doi.org/10.1016/j.jfca.2016.03.004>. Accessed on 8/10/2023.
- [15]Patil, G., Pathmudi, S., Patil, A., 2021, Plant Monitoring System. *International Journal of Engineering Research & Technology (IJERT)*. Vol. 10(9).<http://www.ijert.org>. Accessed on 8/10/2023.
- [16]Saglam, A., Chaerle, L., Van Der Straeten, D., Valcke, R., 2019, Promising monitoring techniques for plant science: Thermal and chlorophyll fluorescence imaging. In *Photosynthesis, Productivity and Environmental Stress*; Wiley: Hoboken, NJ, USA, 2019, 241–266. [CrossRef]. Accessed on 8/10/2023
- [17]Smigaj, M., Gaulton, R., Suárez, J.C., Barr, S.L., 2019, Canopy temperature from an Unmanned Aerial Vehicle as an indicator of tree stress associated with red band needle blight severity. *For. Ecol. Manag.* 2019, 433, 699–708. [CrossRef]. Accessed on 8/10/2023.
- [18]Tucker, C. J., 1979, Red and photographic infrared linear combinations for monitoring vegetation. *Remote sensing of Environment*, 8(2), 127-150. Accessed on 8/10/2023.
- [19]TUİK 2016. http://www.tuik.gov.tr/PreTablo.do?alt_id=1001. <https://biruni.tuik.gov.tr/medas/?kn=92&locale=tr>, Accessed on 8/10/2023.
- [20]UN DESA, 2017, *World Population Prospects: Key findings and advance tables*. New York: UN DESA. Accessed on 8/10/2023.
- [21]Vural, H., Eşiyok, D., Duman, İ., 2000, *Cultivated vegetables (Kültürsebzeleri)*, Ege University press, 440 p. (In Turkish). Accessed on 8/10/2023.
- [21]Woebbecke, D. M., Meyer, G. E., Von Bargen, K., Mortensen, D. A., 1995, Color indices for weed identification under various soil, residue, and lighting conditions. *Transactions of the ASAE*, 38(1), 259-269. Accessed on 8/10/2023.
- [22]Yuan, L., Ju, X., Zhang, L., Wang, J., Yang, Z. N.P.K., 2010, Accumulation in greenhouse soil and its effect on groundwater. *Chin. J. Eco Agric.*, 18, 14–19. (In Chinese) [CrossRef]. Accessed on 8/10/2023.
- [23]Zarco-Tejada, P. J., Berjón, A., López-Lozano, R., Miller, J. R., Martín, P., Cachorro, V., ... & De Frutos, A., 2005, Assessing vineyard condition with hyperspectral indices: Leaf and canopy reflectance simulation in a row-structured discontinuous canopy. *Remote Sensing of Environment*, 99(3), 271-287. Accessed on 8/10/2023.

